JHEP

Published for SISSA by Springer

Received: April 9, 2013
Revised: June 13, 2013
Accepted: June 18, 2013
Published: July 11, 2013

Direct constraints on the top-Higgs coupling from the 8 TeV LHC data

Sanjoy Biswas,[a] **Emidio Gabrielli,**[b,c,1] **Fabrizio Margaroli**[d,a] **and Barbara Mele**[a]

[a] *INFN, Sezione di Roma, c/o Dipart. di Fisica, Università di Roma "La Sapienza", P.le Aldo Moro 2, I-00185 Rome, Italy*

[b] *NICPB, Ravala 10, Tallinn 10143, Estonia*

[c] *INFN, Sezione di Trieste, Via Valerio 2, I-34127 Trieste, Italy*

[d] *Dipart. di Fisica, Università di Roma "La Sapienza", P.le Aldo Moro 2, I-00185 Rome, Italy*

E-mail: sanjoy.biswas@roma1.infn.it, emidio.gabrielli@cern.ch, fabrizio.margaroli@roma1.infn.it, barbara.mele@roma1.infn.it

Abstract: The LHC experiments have analyzed the 7 and 8 TeV LHC data in the main Higgs production and decay modes. Current analyses only loosely constrain an anomalous top-Higgs coupling in a direct way. In order to strongly constrain this coupling, the Higgs-top associated production is reanalyzed. Thanks to the large destructive interference in the t-channel for standard model couplings, this process can be very sensitive to both the magnitude and the sign of a non-standard top-Higgs coupling. We project the sensitivity to anomalous couplings to the integrated luminosity of $50\,\text{fb}^{-1}$, corresponding to the data collected by the ATLAS and CMS experiments in 7 and 8 TeV collisions, as of 2012. We show that the combination of diphoton and multi-lepton signatures, originating from different combinations of the top and Higgs decay modes, can be a potential probe to constrain a large portion of the negative top-Higgs coupling space presently allowed by the ATLAS and CMS global fits.

Keywords: Higgs Physics, Beyond Standard Model, Standard Model

ArXiv ePrint: 1304.1822

[1] On leave of absence from Dipart. di Fisica, Università di Trieste, Strada Costiera 11, I-34151 Trieste, Italy.

doi:10.1007/JHEP07(2013)073

JHEP07(2013)073

Contents

1 Introduction

The discovery of a Higgs-like resonance at the LHC [1, 2] has started up a new phase in the experimental exploration of the electroweak symmetry-breaking (EWSB) mechanism of the standard model (SM). The observed resonance is, within present experimental errors, well compatible with the minimal structure of a Higgs sector. Nevertheless, the determination of different properties of the new particle with increasing precision in the next years of the LHC running is expected to be a powerful mean to explore what could be beyond the SM description of fundamental interactions. In particular, on the one hand, deviations in the new-particle couplings to the electroweak vector bosons $V = W, Z$ would require further degrees of freedom to keep the VV scattering unitary. On the other hand, anomalies in the Yukawa couplings to matter fields could possibly point to a non-standard mechanism for the generation of quark and charged-lepton masses.

With the present moderate statistics collected at 7 and 8 TeV ($\sim 25\,\text{fb}^{-1}$ per experiment), where the main analyses are based on the $H \to \gamma\gamma, ZZ^*, WW^*$ signatures, global fits for the Higgs-like particle couplings are made under simplified assumptions [3, 4, 6]. Similar strategies are followed in Higgs analysis at Tevatron, based on $\sim 10\,\text{fb}^{-1}$ in $p\bar{p}$ collisions at 1.96 TeV [7]. In particular, one can assume a *universal* scale factor C_f (either positive or negative) for the Higgs Yukawa couplings to all fermion species f,

$$Y_f = C_f\, Y_f^{SM}\,, \tag{1.1}$$

JHEP07(2013)073

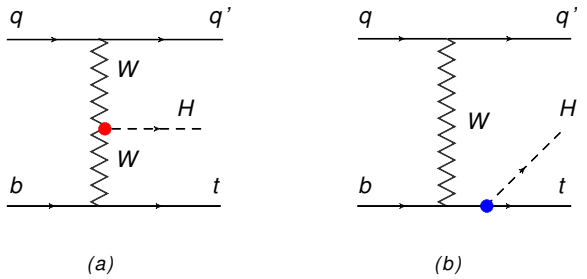

Figure 1. Feynman diagrams for the single-top plus Higgs associated production in the t-channel $q\,b \to t\,q'H$ at hadron colliders. Higgs radiation by the initial b-quark line is neglected.

(where $Y_f^{SM} = m_f/v$ is the SM Yukawa coupling and $v = \langle H \rangle$ is the Higgs vacuum expectation value),[1] and a *universal* (according to custodial symmetry) coupling scale factor C_V to W and Z bosons,

$$C_V = g_{HWW}/g_{HWW}^{SM} = g_{HZZ}/g_{HZZ}^{SM}\,. \tag{1.2}$$

The ATLAS and CMS two-dimensional fits are both compatible within $2\,\sigma$ with a SM coupling setup $C_V = C_f = 1$ [4, 6]. They are likewise compatible with a non-SM setup $C_V \simeq -C_f \simeq 1$. The latter two solutions would be degenerate if it were not for the presence in the production rates of linear terms in C_V and C_f mainly associated to the $H \to \gamma\gamma$ decay width. The latter arise from the (destructive) interference of the top and W loop amplitudes contributing to the decay, and tend to move the second minimum of the (C_V, C_f) likelihood function away from the $C_V \simeq -C_f \simeq 1$ region. It has initially been argued that resolving experimentally this ambiguity by improving the accuracy of the ATLAS and CMS fits will require a larger statistical sample than the present one [8, 9]. More recently, global fits of Higgs couplings tend to disfavor the $C_V \simeq -C_f \simeq 1$ solution [10]–[15]. Nevertheless, the best-fit parameter values seem presently still quite sensitive to statistical fluctuations.

Alternative strategies aimed at excluding more directly the non-standard setup $C_f \simeq -C_V$ have been suggested. In [16, 17], the associated production of a single top quark and a Higgs boson [18]–[20] was proposed as a direct probe of the relative sign of the $Ht\bar{t}$ and HWW couplings at the LHC. In particular, the t channel

$$q\,b \to t\,q'H \tag{1.3}$$

(where the jet originating from the final light quark tends to be at large rapidities) is remarkably sensitive to a change in the C_t relative sign, because of the large destructive interference (proportional to $\sim Y_t\,m_t$) of the two dominant amplitudes of the process in the SM (figure 1) [21]–[23]. By flipping the Y_t sign, the total production cross section for $p\,p \to t\,q\,H$ gets enhanced by a factor ~ 13 over the SM value of ~ 15 (72) fb at 8 (14) TeV

[1] Note that in the SM, the spontaneous EWSB does not fix the overall sign of the Yukawa couplings, which can be rotated away by a chiral transformation of fermion fields. What is observable is the relative sign of the Yukawa coupling and the corresponding fermion mass term in the Lagrangian (predicted as positive in the SM) that is the quantity $sign[Y_f\,m_f]$. In the following, we set the sign of the fermion mass m_f according to the standard notation of the free fermion Lagrangian, and refer to the sign of the Yukawa coupling with respect to the HWW coupling.

JHEP07(2013)073

(summing over t and $\bar{t}$ production),[2] leading to about 0.21 (0.89) pb, for $C_t \simeq -1$ [16]. As a consequence, while a study of the $pp \to tqH$ process in the SM will need quite large integrated luminosities at 14 TeV, the production rates for $C_t \simeq -C_V \simeq -1$ can be large enough to start a direct exploration of the reversed Y_t setup with the integrated luminosity already collected at 7 and 8 TeV.

Note that a change in the Yukawa sign and/or absolute value with respect to its SM value would signal an origin of the fermion masses different from spontaneous EWSB, and spoil the unitarity and renormalizability of the theory [25]. In particular, it was shown in [17] that a change in the relative sign of the Higgs t and W couplings in the $Wb \to tH$ process (the relevant subprocess of the $qb \to tq'H$ scattering) leads to a violation of the perturbative unitarity at a scale $\Lambda \simeq 10$ TeV. This is well above the effective partonic c.m. energies of the tH system involved in the $qb \to tq'H$ production at the LHC (which is at most ~ 1 TeV), and implies that a perturbative calculation of the $qb \to tq'H$ cross section at the LHC collision energies can still be reliable.

In order to assess the LHC potential for detecting an enhancement in the $qb \to tq'H$ cross section, one can exploit different H and t-quark decay channels. As in the main Higgs search processes, considering non-strongly interacting decay products (like in $H \to \gamma\gamma$, $\ell\ell\ell'\ell'$, $\ell\ell'\nu\nu'$ and $t \to qq'b$ or $t \to \ell\nu b$) leads to a reduction in rates, which is more than compensated by the cleaner experimental signatures, that suffer from milder backgrounds.

All Higgs decay branching ratios (BR's) are quite affected by changes in the Yukawa sector. While the $qb \to tq'H$ total cross section is sensitive to the Yukawa sector mostly through the t-quark coupling, the Higgs decay BR's are all sensibly affected also by possible changes in the magnitude of the Higgs couplings to lighter quarks and heavy leptons, notably Y_b, Y_c, Y_τ.[3]

For simplicity, and following the present experimental analysis [3, 4, 6], we will assume from now on either a *universal* scale factor C_f (varying in the range $-1.5 \lesssim C_f \lesssim 1.5$) for all fermion species f, or a scale factor C_t parametrizing the top Yukawa coupling, with $C_f = 1$ for all lighter fermions.[4] As for the HVV couplings, we will allow for a variation of a few 10% around the SM value $C_V = 1$.

In [16], a study of the potential of the $qb \to tq'H$ channel for revealing a non-standard Yukawa sign was made, exploiting the two-photon signature for the Higgs decay accompanied by hadronic top decays plus a forward jet

$$q\,b \to t\,q'\,H \to (b\,qq')\,q'\,\gamma\gamma\,. \tag{1.4}$$

A parton-level simulation, including the main irreducible backgrounds, in the universal C_f hypothesis, found that at 14 TeV, for $-1.5 \lesssim C_f \lesssim 0$, an integrated luminosity of 60 fb^{-1} would give about 10 signal events versus less than 0.3 background events, with a corresponding signal significance at a 3-σ level. At 8 TeV, with same integrated luminosity, the corresponding significance drops to around 1.5 σ.

[2] Note that NLO QCD corrections increase the SM cross sections by about 15% [17, 24].

[3] A change in the sign of the latter couplings would be nevertheless ineffective in this case.

[4] In both cases, loop-induced processes are assumed to scale according to the SM loop structure.

JHEP07(2013)073

In [17], the potential of $p\,p \to t\,q\,H$ was assessed through the hadronic $H \to b\bar{b}$ decay, focussing on the quite challenging 3-b and 4-b signatures, and semileptonic t decay

$$q\,b \;\to\; t\,q'\,H \to\; (\ell\,\nu\,b)\,q'\,b\,\bar{b}\,, \qquad q\,g \to\; t\,q'\,H\,b \to\; (\ell\,\nu\,b)\,q'b\,\bar{b}\,b\,. \tag{1.5}$$

In the universal C_f hypothesis, it turns out that $50\,\text{fb}^{-1}$ at 14 TeV could be sufficient to exclude the negative C_f range presently allowed by experimental fits, while at 8 TeV the same integrated luminosity would only partially exclude this possibility. On the other hand, after switching to a non-universal C_t scaling with $C_b = C_c = C_\tau = 1$, the reach of the $H \to \bar{b}b$ channel is enhanced in the region $|C_t| \lesssim 1$, because of the corresponding relative increase in the $H \to \bar{b}b$ width.

The aim of the present analysis is to extend our previous study of the $q\,b \to t\,q'H$ channel in [16] in order to assess its potential for the exclusion of a non-standard Yukawa sign with the statistics presently accumulated at 7 TeV and 8 TeV at the LHC. We present a parton-level analysis including the most robust signatures, corresponding to either photon pairs or more than one lepton in the final states, for which the rate suppression by the corresponding Higgs decay BR is expected to be compensated by a better signal-to-background ratio S/B. The latter signatures are associated to the decays

$$H \to \gamma\gamma\,, \quad H \to WW^* \to \ell\nu\ell'\nu,\; \ell\nu\,qq'\,, \quad H \to \tau\tau \to \ell\nu\nu\,\ell'\nu\nu,\; \ell\nu\nu + had(s)\,, \tag{1.6}$$

which, in the $C_f \lesssim 0$ case, are expected to be statistically relevant in the $q\,b \to t\,q'H$ production with the present LHC data set. In particular, on the one hand, we complement the $H \to \gamma\gamma$ analysis for a hadronic top decay [cf. eq. (1.4)] carried out in [16] with the one with a semi-leptonic top decay, requiring two photons plus a charged lepton in the final state

$$q\,b \to\; t\,q'\,H \to\; (\ell\,\nu\,b)\,q'\,\gamma\gamma\,. \tag{1.7}$$

On the other hand, we consider now also: *i)* the three-lepton signature arising from the semi-leptonic top decay combined with the decays $H \to WW^* \to \ell\nu\ell'\nu$, and $H \to \tau\tau \to \ell\nu\nu\,\ell'\nu\nu$, and *ii)* the two-same-sign-lepton signature arising from the semi-leptonic top plus the decays $H \to WW^* \to \ell\nu\ell'\nu$, $\ell\nu\,qq'$, and $H \to \tau\tau \to \ell\nu\nu\,\ell'\nu\nu$, $\ell\nu\nu + had(s)$, leading to the following final states

$$q\,b \;\to\; t\,q'\,H \to\; (\ell\,\nu\,b)\,q'\,\ell\,\ell' + \nu' s\,, \qquad q\,b \;\to\; t\,q'\,H \to\; (\ell\,\nu\,b)\,q'\,\ell + \nu' s + X_h\,, \tag{1.8}$$

where X_h is made of further hadronic states either from the W or the τ hadronic decays. In the present analysis, we closely follow the approach in [16], and estimate the corresponding main *irreducible* (and *reducible* for the diphoton channel) backgrounds at parton level, requiring the tagging of a b-jet in the final state (arising from the top decay), plus a forward light jet.[5]

We will show that, using the present LHC statistics, the $H \to \gamma\gamma, WW^*, \tau\tau$ decays in $p\,p \to t\,q\,H$ have a strong potential to exclude in a direct way most of the $C_f \lesssim 0$ region in the (C_V, C_f) plane which is allowed by the present ATLAS and CMS Higgs-coupling fits.

[5] Reducible backgrounds are expected to be subdominant for the multilepton signatures considered here.

JHEP07(2013)073

As expected, the exclusion power of the photon-pair and multi-lepton signatures (excluding the $H \to \tau\tau$ component) turns out to be complementary to the $H \to b\bar{b}$ decay, the corresponding rates being enhanced when $|C_b| \lesssim 1$, where the $H \to b\bar{b}$ signal rates are depleted.

The plan of the paper is the following. In section 2, we detail the (C_V, C_f) dependence of the $p\,p \to t\,q\,H$ production cross sections, and the corresponding signal event rates for the $H \to \gamma\gamma, WW^*, \tau\tau$ decays. In section 3, we describe the relevant SM backgrounds and selection cuts for the processes in eqs. (1.7) and (1.8), and recall the relevant results of our previous study for eq. (1.4). For a data set of $50\,\text{fb}^{-1}$, we present for each signature the event numbers (S) for signals in different channels versus $C_t = 0, \pm 1$ (and $C_V = 1$), the background event numbers (B), and the corresponding expected significance. In section 4, we combine our findings, and show the expected exclusion regions in the (C_V, C_f) plane, both in the universal Yukawa scaling assumption, and in the hypothesis of C_t scaling with $C_{f\neq t} = 1$. In section 5, we draw our conclusions.

2 Signal production rates versus C_V and C_f

In this section, we present the $p\,p \to t\,q\,H$ cross-section and $BR(H \to \gamma\gamma, WW^*, \tau\tau)$ dependence on the C_f and C_V scaling factors through the corresponding enhancement factors R_i with respect to the SM predictions. In particular, we will detail the behavior of the quantities

$$R_\sigma = \frac{\sigma}{\sigma^{SM}}\ , \qquad R_{BR_{\gamma\gamma,WW,\tau\tau}} = \frac{BR_{\gamma\gamma,WW,\tau\tau}}{(BR_{\gamma\gamma,WW,\tau\tau})^{SM}}\ . \tag{2.1}$$

By combining the latter, we get the signal strength for the corresponding decay channel

$$R_{\sigma\cdot BR_{\gamma\gamma,WW,\tau\tau}} = \frac{\sigma \cdot BR_{\gamma\gamma,WW,\tau\tau}}{(\sigma \cdot BR_{\gamma\gamma,WW,\tau\tau})^{SM}}\ , \tag{2.2}$$

that will primarily affect the signal event number dependence on the C_f and C_V scaling factors. A further moderate coupling dependence will arise from the efficiencies of actual kinematic cuts in the final event selection (cf. section 3).

We will make two different assumptions for the Yukawa coupling variation:

- *Universal Yukawa rescaling*, which assumes just one free parameter $C_f = C_t$ describing all Yukawa couplings both in production and decay amplitudes. Varying the top-quark coupling C_t will then largely affect not only the production cross section, but also the Higgs branching ratios $BR_{\gamma\gamma}$, BR_{WW} and $BR_{\tau\tau}$. The main effect of the C_f variation on BR_{WW} will arise from the Higgs total width dependence on the Higgs couplings to the b quark and lighter fermions. On the other hand, in $BR_{\gamma\gamma}$ there will be a further non-trivial dependence on C_t caused by the top-quark loop that in the SM interferes destructively with the W loop in the $H \to \gamma\gamma$ amplitude.

- *Free C_t and $C_{f\neq t} = 1$*, with C_t affecting mainly the production cross sections and the $H \to \gamma\gamma$ width, while leaving almost unaltered BR_{WW} and $BR_{\tau\tau}$.

JHEP07(2013)073

In the following, all numerical cross sections will refer to the hadronic pp collisions (even when the *partonic* initial state is shown). The production rates at leading order have been computed via the MadGraph 5 (v1.3.33) software package [26], and the CTEQ6L1 parton distribution functions [27]. Both the factorization and renormalization scales are set at the value $Q = \frac{1}{2}(m_H + m_t)$ for the $pp \to t\,q\,H$ signal, where m_t is the top-quark mass. The other relevant parameters entering our computation are set as follows [1, 2, 28, 29]: $m_H = 125$ GeV, $m_t = 173.2$ GeV, $M_Z = 91.188$ GeV, $M_W = 80.419$ GeV, $m_b = 4.7$ GeV, and $\alpha_S(M_Z) = 0.118$.

The $BR_{\gamma\gamma}$, BR_{WW} and $BR_{\tau\tau}$ values versus the C_f and C_V scaling factors have been obtained through an original code we have built up, containing all the leading corrections (including off-shellness effects for both W's in the decay $H \to W^*W^*$).[6]

For reference, the *SM* $pp \to t\,q\,H$ cross section (summing up contributions from the two charge-conjugated channels)[7] is

$$\sigma(q\,b \to t\,q'H)^{SM} \simeq 15.2 \text{ fb} \qquad \text{at} \quad \sqrt{s} = 8 \text{ TeV} \,, \tag{2.3}$$

and the *SM* Higgs branching ratios $BR_{\gamma\gamma}$, BR_{WW} and $BR_{\tau\tau}$, that are relevant in the following, are

$$BR^{SM}_{\gamma\gamma} \simeq 2.30 \cdot 10^{-3} \,, \qquad BR^{SM}_{WW} \simeq 0.209 \,, \qquad BR^{SM}_{\tau\tau} \simeq 6.55 \cdot 10^{-2} \,. \tag{2.4}$$

Note that, for $C_V = 1$, the total Higgs width Γ_H drops, for vanishing C_t, from its *SM* value $\Gamma_H(C_t = \pm 1) \simeq 4.04\,\text{MeV}$ to $\Gamma_H(C_t = 0) \simeq 0.955\,\text{MeV}$, assuming a universal scaling in C_f.

In figure 2 we show (for the three values $C_V = 1, 0.7, 1.3$, from top to bottom) the dependence on C_t of the enhancement factors R_i , as defined in eq. (2.1), for $BR_{\gamma\gamma}$, BR_{WW}, $BR_{\tau\tau}$ (left), and the corresponding signal strengths, as defined in eq. (2.2), at $\sqrt{s} = 8\,\text{TeV}$ (right). The red, blu, black lines refer to the $H \to \gamma\gamma$, WW^*, $\tau\tau$ channels respectively. Plots in figure 2 correspond to the *universal scaling* scenario $C_f = C_t$. In figure 3, we show the same plots as in figure 2, but for the C_t scaling scenario with $C_{f\neq t} = 1$. In the right plots of figures 2 and 3, we also show the corresponding enhancement for the basic $pp \to t\,q\,H$ total cross section (dashed lines) normalized to the SM, versus C_t.

Throughout the paper, we focus on the range

$$-1.5 < C_t < 1.5 \,, \tag{2.5}$$

where the C_t dependence is more critical, and the most favored regions of the LHC fits lie [4, 6]. In the universal scaling scenario (cf. figures 2, left), the $R_{BR_{\gamma\gamma}}$ and $R_{BR_{WW}}$ behavior is clearly driven by the Γ_H reduction for $|C_f| \to 0$, with asymmetric corrections due to interference effects enhancing $R_{BR_{\gamma\gamma}}$ for negative C_t.

[6] We checked that its results for the SM case match the HDECAY [30] predictions within a few per-cent.

[7] The contribution to the $pp \to t\,q\,H$ cross section of the amplitude where the Higgs is radiated by the initial b-quark line is small (at the per-mil level in the C_t range relevant here), and will be neglected in the present analysis.

JHEP07(2013)073

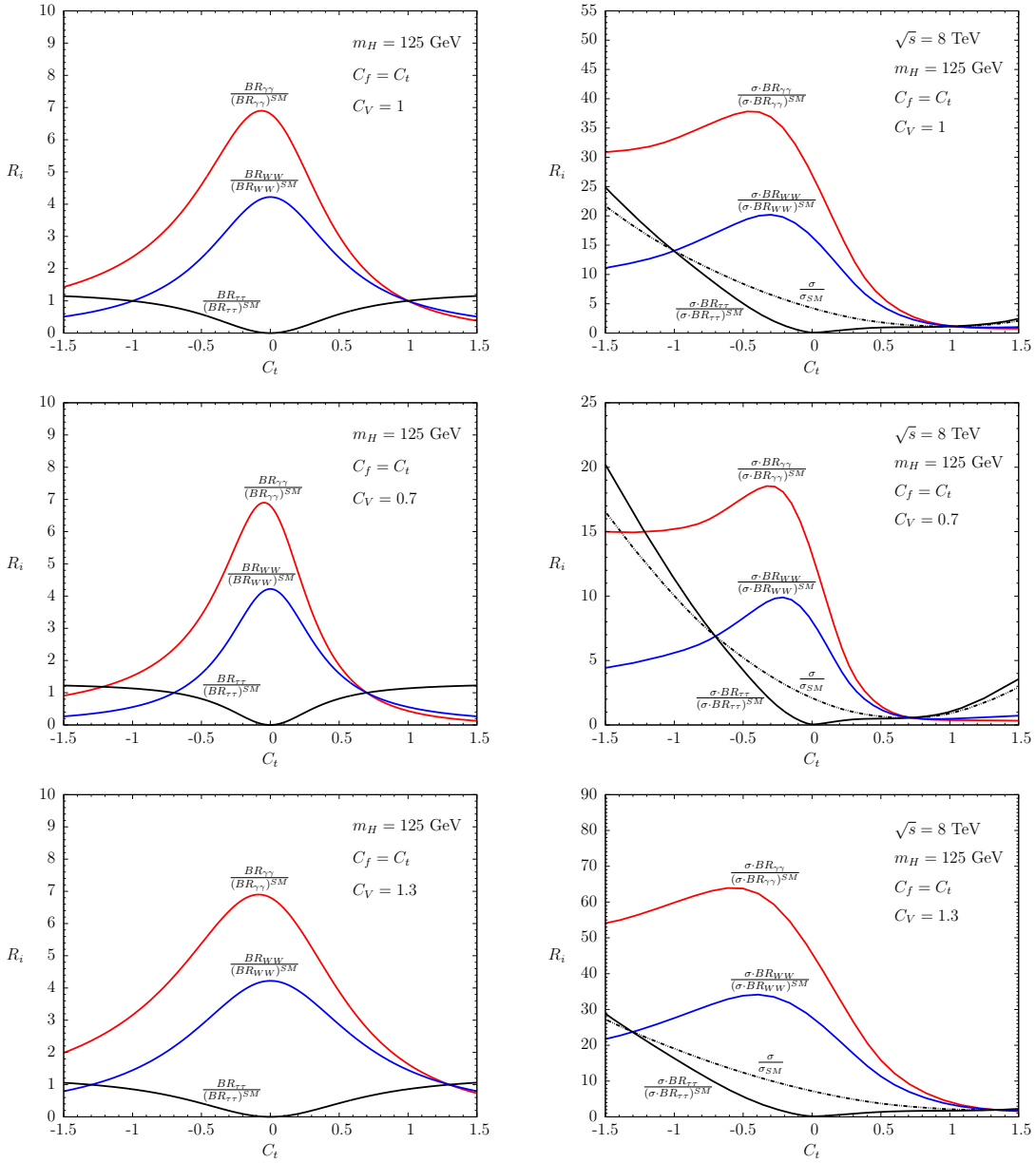

Figure 2. Enhancement factors R_i versus C_t, normalized to the SM, for the branching ratios $BR_{\gamma\gamma}$, BR_{WW}, and $BR_{\tau\tau}$ (left), and the corresponding signal strengths as defined in eq. (2.2) (right), for $\sqrt{S} = 8\,\text{TeV}$, and for the universal scaling scenario $C_f = C_t$. Dashed lines in the right plots correspond to the $pp \to tqH$ total cross section σ normalized to the SM one. Plots from top to bottom correspond to $C_V = 1, 0.7, 1.3$, respectively.

In the $C_{f\neq t} = 1$ scenario (cf. figures 3, left), $R_{BR_{\gamma\gamma}}$ and $R_{BR_{WW}}$ are definitely less sensitive to C_t, with the dominant effect deriving from the positive interference effects in $R_{BR_{\gamma\gamma}}$ for $C_t < 0$.

An even more dramatic enhancement for negative C_t is present in the $p\,p \to t\,q\,H$ production cross section. When combined with the $R_{BR_{\gamma\gamma}}$ and $R_{BR_{WW}}$ behavior

JHEP07(2013)073

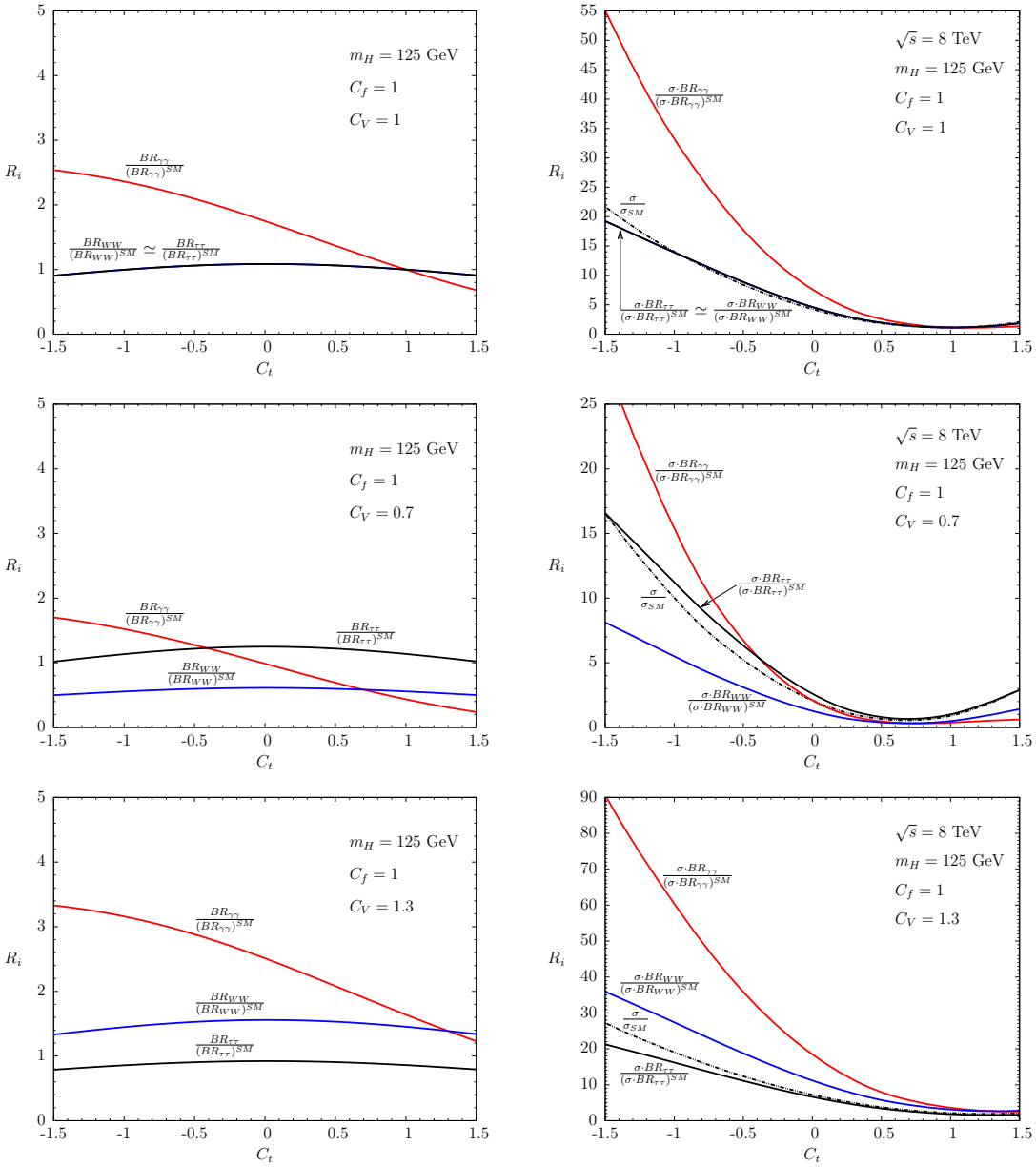

Figure 3. Same as in figure 2, but for the C_t scaling scenario with $C_{f\neq t} = 1$.

for universal C_f scaling (cf. figures 2, right), the latter tends to level up the dependence on C_t of the corresponding signal strengths in the negative C_t region.

On the other hand, in the $C_{f\neq t} = 1$ scenario, the signal strengths follows a (less involved) monotonic behavior.

The parameter dependence just shown will be crucial in the following analysis to understand the exclusion potential of the $p\,p \to t\,q\,H$ process in the (C_V, C_f) plane.

JHEP07(2013)073

3 Single top quark and Higgs boson production

In [16], we estimated the sensitivity to an anomalous $p\,p \to t\,q\,H$ production focussing on the events where the Higgs boson decays to photons, and the top quark decays hadronically. The study was based on an integrated luminosity of $60\,\text{fb}^{-1}$ at 8 TeV and 14 TeV. Here the same estimate is repeated for the approximate $50\,\text{fb}^{-1}$ collected by the ATLAS and CMS experiments in the 7 and 8 TeV LHC runs (in particular $\sim 5\,\text{fb}^{-1}$ at 7 TeV plus $\sim 20\,\text{fb}^{-1}$ at 8 TeV, for each experiment). Different Higgs-boson and top-quark decays will be analyzed in several non-overlapping final states. The sensitivity of all independent decay channels of the $p\,p \to t\,q\,H$ final state will be thus assessed separately.

3.1 $H \to \gamma\gamma$

Here, we first update our previous sensitivity estimate on the basis of the total luminosity collected so far in the 7 and 8 TeV LHC runs. In addition, we analyze for the first time the sensitivity of the final state where $t \to b\,\ell\nu$. Throughout the paper, a lepton ℓ is assumed to be either an electron or a muon.

3.1.1 Final state with a hadronically decaying top quark

The hadronic top quark decays allow the full reconstruction of the event kinematics. Combinatorics in the jet-to-parton assignment is greatly reduced by the usage of b-tagging algorithms, and by the requirement that the most forward jet be the one not emerging from the top quark decay. The irreducible SM backgrounds include top and multi-jet final states, all accompanied by two high-p_T photons,

- $pp \to 2\,\gamma + t + j$;
- $pp \to H(\to \gamma\gamma) + t\bar{t}$;
- $pp \to 2\,\gamma + \bar{t}\,t$;
- $pp \to 2\,\gamma + b + 3\,j$.

We include also the top-pair and Higgs associated production $pp \to t\bar{t}H$ as a relevant background in all channels, taking into account the $Ht\bar{t}$ coupling dependence for consistency (notably giving a null contribution to the background in the $C_t = 0$ case). Among the reducible backgrounds the dominant contribution comes from $pp \to 2\,\gamma + 4\,j$, where one of the light jets can be mistagged as a b-jet. We assume a b-jet identification efficiency of 60%, with a corresponding fake jet rejection factor of 10 for c-jet, and 100 for other light jets.

For the present channel, we retain only the events passing the following selection criteria on the transverse momentum p_T and pseudo rapidity η of the final state particles:

$$p_T^{\gamma_1} > 40\,\text{GeV}, \qquad p_T^{\gamma_2} > 30\,\text{GeV}, \qquad p_T^{j,b} > 25\,\text{GeV}, \qquad |\eta_{\gamma,b}| < 2.5, \qquad |\eta_j| < 4.5. \quad (3.1)$$

The above cuts reflect the requirement imposed by the ATLAS and CMS di-photon triggers, and fiducial regions of the detectors for the final state objects.

JHEP07(2013)073

$\sqrt{s} = 8\,\text{TeV}$ $(50\,\text{fb}^{-1})$	*Signal (S)*			*Background (B)*				
Cut	$C_t = -1$	$C_t = 0$	$C_t = 1$	$2\gamma\, tj$	$2\gamma\, t\bar{t}$	$t\bar{t}H$	$2\gamma\, b\, 3j$	$2\gamma\, 4j$
$2\gamma + b + (\geq 3\, j)$	6.4	5.1	0.18	8.2	9.2	1.6	249	1263
$\lvert\eta_{j_F}\rvert > 2.5$ & $p_{T_{j_F}} > 30\,\text{GeV}$	3.0	2.5	0.08	3.3	0.32	0.06	22	116
$\lvert M_{bjj} - m_t\rvert < 20\,\text{GeV}$	3.0	2.4	0.08	3.3	0.20	0.02	4.5	30
$\lvert M_{jj(top)} - M_W\rvert < 15\,\text{GeV}$	2.8	2.3	0.07	3.2	0.19	0.02	1.8	4.6
$\lvert M_{\gamma\gamma} - m_H\rvert < 3\,\text{GeV}$	2.8	2.3	0.07	0.12	0.02	0.02	0.57	0.26
$S/\sqrt{S+B}$	1.4	1.3	0.07					

Table 1. Number of events passing sequential cuts for the signal $pp \to t\,q\,H \to t\,q\,\gamma\gamma$ and SM backgrounds at $\sqrt{s} = 8\,\text{TeV}$, with integrated luminosity of $50\,\text{fb}^{-1}$, assuming $C_f = C_t$. Results correspond to $m_H = 125\,\text{GeV}$. An estimate of the sensitivity of this channel to the signal, given by the significance $S/\sqrt{S+B}$ (with B summed up over all contributions), is shown in the lowest row. The contribution of $t\bar{t}H$ to the SM background has been set to zero in the evaluation of $S/\sqrt{S+B}$ at $C_t = 0$.

In all our analysis, we use the following general isolation requirement for any pair of objects in the final state

$$\Delta R_{i,j} = \sqrt{\Delta\eta_{i,j}^2 + \Delta\phi_{i,j}^2} > 0.4\,, \tag{3.2}$$

with i and j running over all the final particles and jets (including b-jets), $\Delta\eta$ being the rapidity gap, and $\Delta\phi$ the azimuthal-angle gap between any particle pair.

For the present channel, the highest rapidity light-jet in the final state is required to have $|\eta| > 2.5$ and $p_T > 30$ GeV. For all other final states this condition will be somewhat relaxed, thanks to the presence of more characterized final states with extra charged leptons.

As in our previous study, we require the top quark to be fully reconstructed in the hadronic mode, with the invariant mass of the remaining 3-jets system (out of which one is a b-jet) peaking at the top quark mass, within a mass window consistent with the ATLAS and CMS jet energy resolution, i.e. 20 GeV. Then, the invariant mass of the two light jets contributing to the top quark invariant mass, is required to peak at the W mass within a mass window of 15 GeV. Finally, the invariant mass of the di-photon system is imposed to reconstruct the Higgs mass centered at 125 GeV within a mass resolution of ± 3 GeV.

The results of the above selection procedure are shown in table 1 for $m_H = 125\,\text{GeV}$, $\sqrt{s} = 8\,\text{TeV}$, and integrated luminosity of $50\,\text{fb}^{-1}$. The numbers of events passing the sequential cuts defined above are reported for the $pp \to t\,q\,H \to t\,q\,\gamma\gamma$ signal with hadronic top decay, for different $C_t = \pm 1, 0$ values (assuming $C_f = C_t$ in $BR_{\gamma\gamma}$), for the main irreducible backgrounds, and one reducible background. The first row refers to the total number of events that pass the photon- and jet-tagging definition. As anticipated, we include in our analysis of the relevant backgrounds the $t\bar{t}H$ final state, for all the Higgs decay channels considered. This will give rise to a mild dependence on C_t of the total background rates in the range of C_t values considered here. The results explicitly shown in the

JHEP07(2013)073

tables 1-4 for different channels is the total number of $t\bar{t}H$ background events corresponding to $C_t = \pm 1$. However, in the evaluation of the significance at $C_t \neq 1$, we consistently tune the $t\bar{t}H$ event rates in the total background. We also estimated the contribution from the reducible background $2\,\gamma + b\bar{b} + 2\,j$, where one of the b-quark is mistagged as a light jet. The latter is found to be quite small after applying the set of cuts in table 1, contributing by about 0.01 events (corresponding to a cross section of $2.0 \cdot 10^{-4}$ fb at 8 TeV).

From these results, we can see the efficiency of the different cuts applied to enhance the signal-to-background ratio. In particular, the signal rate is mainly affected by the forward-jet tag requirement, with a corresponding reduction of roughly a factor 2, and it passes almost unaltered the remaining cuts. The largest contribution to the background comes from the $2\,\gamma + b + 3\,j$ non-resonant final state. This is considerably affected by both the forward-jet cut and the top- and Higgs-resonance requirements. The same holds for the reducible $2\,\gamma + 4\,j$ background,[8] which contributes by almost 50% of the $2\,\gamma + b + 3\,j$ event rate. The next background for relevance is the single-top production $2\,\gamma + t + j$, while the top-pair channels $2\,\gamma + \bar{t}\,t$ and $H(\to 2\,\gamma) + \bar{t}\,t$ contribute to the total rate of background events negligibly. Finally, in the bottom row of table 1, we report an estimate of the sensitivity of this channel to an anomalous C_t value, given by the significance defined as $S/\sqrt{S+B}$, for $C_t = -1, 0, 1$.

3.1.2 Final state with a leptonically decaying top quark

We now consider the $p\,p \to t\,q\,H \to t\,q\,\gamma\gamma$ process, in events where the top quark decays leptonically $t \to b\,\ell\,\nu$, and $\ell = e, \mu$. The irreducible backgrounds are given by the processes

- $pp \to 2\,\gamma + t + j$;
- $pp \to H(\to \gamma\gamma) + t\bar{t}$;
- $pp \to 2\,\gamma + \bar{t}\,t$;
- $pp \to 2\,\gamma + W + b + j$.

The dominant reducible background $pp \to 2\,\gamma\,W\,2\,j$ has also been included where one of the light jet is mistagged as a b-jet.

In addition to the isolation criteria in eq. (3.2), the following selection cuts have been applied on the final state particles:

$$p_T^\gamma > 20\,\text{GeV}, \quad p_T^\mu > 20\,\text{GeV}, \quad p_T^{e,j,b} > 25\,\text{GeV}, \quad |\eta_{\gamma,l,b}| < 2.5, \quad |\eta_j| < 4.5. \tag{3.3}$$

Here, the looser cuts on the photon transverse momentum p_T^γ are allowed by the addition of a single-lepton trigger. The most forward jet j_F is required to have a pseudo-rapidity of at least 1.5. As the dominant backgrounds also feature leptonically decaying top quarks, we do not attempt for a partial top-quark reconstruction.

In table 2, we show our results for the event yields for the signal and different backgrounds, for the representative $C_t = -1, 0, 1$ values. From the latter results, it can be

[8] In this case, after mistagging one of the light jet as a b-jet and tagging a forward jet out of the remaining 3 jets, the fake b-jet has been combined with the remaining two jets to form the top system.

JHEP07(2013)073

$\sqrt{s} = 8\,\text{TeV}$ $(50\,\text{fb}^{-1})$	*Signal (S)*			*Background (B)*				
Cut	$C_t = -1$	$C_t = 0$	$C_t = 1$	$2\gamma\, tj$	$2\gamma\, t\bar{t}$	$t\bar{t}H$	$2\gamma\, W\, bj$	$2\,\gamma W 2\, j$
$2\gamma + \ell + b + (\geq \text{j})$	3.01	2.35	0.08	7.0	6.5	0.8	5.0	5.57
$\lvert M_{\gamma\gamma} - m_H \rvert < 3\,\text{GeV}$	3.01	2.35	0.08	0.16	0.18	0.77	0.09	0.12
$\lvert \eta_{j_F} \rvert > 1.5$	2.54	2.01	0.06	0.12	0.04	0.15	0.03	0.04
$S/\sqrt{S+B}$	1.5	1.3	0.09					

Table 2. Same as in table 1 for the signal $p\,p \to t\,q\,H \to t\,q\,\gamma\gamma$, and SM backgrounds, but for the top quark decaying leptonically.

seen that, by using as simple figure of merit $S/\sqrt{S+B}$, the sensitivity that can be achieved in this class of events is comparable to the one where the top quark decays hadronically.

3.2 $H \to WW^*$ and $H \to \tau\tau$

Several combinations of number and charge of leptons are available in the $p\,p \to t\,q\,H \to bWqWW, bWq\,\tau\tau$ final states. We will narrow our study to the ones that are of larger potential in terms both of sensitivity to a signal, and in robustness against poorly known backgrounds, i.e. events where at least two W's or two τ's (or one W and one τ) decay leptonically. As $BR(H \to \tau\tau)$ is approximately a factor 3 smaller than $BR(H \to WW^*)$, in the SM, and the τ branching ratio in electrons/muons is larger than $BR(W \to e(\mu)\,\nu)$, the final states with multi leptons will in general be sensitive to a mixture of W and τ. The W's (both in signal and in backgrounds) are let to decay only to the leptons of first two generations. On the other hand, the tau decay in the $H \to \tau\tau$ signal has been handled using the in-built interface in the event generator PYTHIA [31].[9] We assume the same isolation criteria for the leptons coming from the W and tau decays.

3.2.1 Final state with three charged leptons

The final state in this case is $3\,\ell + b + j$ (with $\ell = e$ or μ). Two of the three leptons have their origin from the decays of two W's or τ's coming from the Higgs decay, and the additional prompt lepton comes from the top semileptonic decay. The irreducible backgrounds which contribute to this final state are:

- $pp \to t\bar{t} + W$;
- $pp \to t\bar{t} + Z$;
- $pp \to t\bar{t} + H$;
- $pp \to t + WW + j$;
- $pp \to t + WZ + j$;

[9] Though we are working with parton-level jets, for the hadronic tau decay, the decay products have been considered as a single jet in our analysis.

JHEP07(2013)073

$\sqrt{s} = 8\,\text{TeV}$ $(50\,\text{fb}^{-1})$	*Signal (S)*			*Background (B)*				
Cut	$C_t = -1$	$C_t = 0$	$C_t = 1$	$t\bar{t}W$	$t\bar{t}Z$	$t\bar{t}H$	$tWWj$	*Total*
$\ell_i^\pm \ell_i^\pm \ell_j^\mp bq$	0.96	0.81	0.06	3.69	0.14	1.07	0.04	4.94
$\lvert\eta_j^F\rvert > 1.5$	0.81	0.70	0.05	0.64	—	0.18	0.01	0.83
$S/\sqrt{S+B}$	0.63	0.57	0.05					
	Signal (S)			*Backgrounds (B)*				
	$C_t = -1$	$C_t = 0$	$C_t = 1$	$t\bar{t}W$	$t\bar{t}Z$	$t\bar{t}H$	$tWWj$	*Total*
$\ell_i^\pm \ell_j^\pm \ell_j^\mp bq$	3.11	2.58	0.18	12.2	43.5	3.3	0.2	59.2
$\lvert\eta_j^F\rvert > 1.5$	2.72	2.22	0.14	2.6	11.0	0.6	0.1	14.3
$M_{\ell_j^+\ell_j^-} \notin [86.2, 96.2]\,\text{GeV}$	2.16	1.76	0.11	2.0	0.2	0.4	—	2.6
$S/\sqrt{S+B}$	0.99	0.88	0.07					

Table 3. Same as in table 1, but for the signal $p\,p \to t\,q\,H$, with $H \to \ell\nu(\nu)\ell\nu(\nu)$ and $t \to b\ell\nu$, and corresponding irreducible backgrounds.

- $pp \to b + WZ + j$;
- $pp \to b + WWZ$.

We impose the following event selection criteria

$$N_\ell = 3 \qquad p_T^\ell > 20\,\text{GeV}, \qquad p_T^{(j,b)} > 20\,\text{GeV} \qquad |\eta_{\ell,b}| < 2.5, \qquad |\eta_j| < 4.5 \ , \quad (3.4)$$

which has a large acceptance to the signal, while keeping large rejection for the above backgrounds. Similarly to the other channels investigated, all final state particles are required to be sufficiently isolated by imposing the isolation criteria in eq. (3.2). A rapidity cut $|\eta| > 1.5$ on the forward jet has also been applied.

In connection to differences in the backgrounds, it is useful to discriminate among two different sets of tri-lepton signatures, depending on the combination of charges and flavors of the leptons. In particular:

- $e^\pm e^\pm \mu^\mp$ and $\mu^\pm \mu^\pm e^\mp$ signatures, where out of three leptons, two leptons have the same charge and same flavor, while the third one has opposite charge and different flavor. This final state is defined here as $\ell_i^\pm \ell_i^\pm \ell_j^\mp + b + jets$ (with $i \neq j$).
- The complementary signature to the above 3-lepton one, defined as $\ell_i^\pm \ell_j^\pm \ell_j^\mp + b + jets$.

A large fraction of the background is characterized by the emission of a Z vector boson in place of the Higgs boson. Then, in order to suppress the latter backgrounds, the invariant mass of two opposite-sign (same-flavor) leptons is required to be $M_{\ell^+\ell^-} \notin [86.2, 96.2]$.

In table 3, we show our results for the event yields, under three different C_t assumptions, and the corresponding background yields. The extra background contribution coming from $tWZ, bWZj, bWWZ$ processes, arising in events where the opposite sign

JHEP07(2013)073

$\sqrt{s} = 8\,\text{TeV}$ $(50\,\text{fb}^{-1})$	*Signal (S)*			*Backgrounds (B)*					
Cut	$C_t = -1$	$C_t = 0$	$C_t = 1$	$t\bar{t}W$	$t\bar{t}Z$	$t\bar{t}H$	$tWWj$	$tW\,3j$	*Total*
$\ell^\pm\ell^\pm bqqq$	7.8	6.3	0.53	45.1	3.7	8.4	0.5	0.3	57.9
$\lvert\eta_j^F\rvert > 1.5\,\text{GeV}$	6.6	5.4	0.42	11.3	0.6	1.8	0.2	0.1	13.9
$S/\sqrt{S+B}$	1.5	1.3	0.11						

Table 4. Same as in table 1, for the signal and corresponding irreducible background numbers of events, but for final states with two same-sign leptons.

leptons share the same flavor, is effectively suppressed to a negligible level once the Z mass veto is applied. The relative contribution of $p\,p \to t\,q\,H$ with $H \to WW^*$ and $H \to \tau\tau$ to the tri-lepton signal is approximately 2 to 1.

3.2.2 Final state with two same-sign leptons

The final state in this case is $\ell^\pm\ell^\pm b\,qqq$ (with $\ell = e$ or μ). In order to achieve the same-sign dilepton production, one of the charged leptons must arise from the top decay, while the other from the leptonic decay of the W(or τ) that shares the sign with the W coming from the top quark. The main backgrounds in this channel are, in order of importance:

- $pp \to t\bar{t} + W$;
- $pp \to t\bar{t} + Z$;
- $pp \to t\bar{t} + H$;
- $pp \to t + WW + j$;
- $pp \to t + W + jjj$.

The possible acceptance of the adopted event selection to the $bWW3j$ and $bbWW2j$ final states has been investigated, and found to be negligible once normalized to the $50\,\text{fb}^{-1}$ of integrated luminosity at 8 TeV collisions.

The following event selection has been adopted, according to present experimental analysis in the same-sign dilepton final state [32]

$$N_\ell = 2 \qquad p_T^\ell > 20\,\text{GeV}, \qquad p_T^{(j,b)} > 20\,\text{GeV} \qquad |\eta_{\ell,b}| < 2.5, \qquad |\eta_j| < 4.5\,, \quad (3.5)$$

with the requirement that the two charged leptons are either both positively or both negatively charged. A rapidity cut $|\eta| > 1.5$ on the forward jet has been applied. The corresponding results for the signal and background events are reported in table 4.

The relative weight of $H \to WW^*$ and $H \to \tau\tau$ contributions to the $p\,p \to t\,q\,H$ final state is again approximately 2 to 1.

JHEP07(2013)073

4 Sensitivity to anomalous Yukawa couplings

After assessing the sensitivity to an anomalous single-top plus Higgs production in different final states, we proceed to study their combined potential, and the implications on the parameter space of the Higgs couplings in the two scenarios highlighted in section 2. We thus combine the five channels discussed in section 3, i.e. events with $H \to \gamma\gamma$ and top decaying either leptonically or hadronically, the two tri-lepton final states (i.e. the set with same-sign same-flavor lepton pairs, and the complementary set), and the same-sign dilepton final states, the latter three channels being simultaneously sensitive to $H \to WW^*$ and $H \to \tau\tau$. As previously, we exploit the full LHC luminosity collected at 7 and 8 TeV by ATLAS and CMS.

Table 5 presents a summary of the signal event numbers (S), background event numbers (B), and corresponding significances $S/\sqrt{S+B}$, for the five channels considered, versus C_t (for the values $C_t = -1.5, -1, 0, 0.3$) in the universal scaling scenario ($C_f = C_t$), with $C_V \simeq 1$. It is straightforward to see that the signal-rate (and corresponding significance) profile for each channel closely follows the signal-strength behavior in figure 2. The latter leads to a roughly constant magnitude for both signal rates and significances for $C_t \lesssim 0$. The dominant contributions come from the two $\gamma\gamma$ channels (with comparable strength), and the two-same-sign lepton channel, each contributing by a 1.5-σ significance at $C_t \sim -1$ (the latter channel having larger event numbers which are compensated by higher background rates). Note that in the multi-lepton components, the $H \to WW^*$ contribution would provide a comparatively good signal rate *closer* to the $C_t \sim 0$ region with respect to the $\gamma\gamma$ channels (cf. figure 2). The latter behavior is actually compensated by the $H \to \tau\tau$ component of the multi-lepton channels (giving on average 30% of the total multi-lepton rates), which rapidly drops for $C_t \to 0$. Altogether, the total significance approaches the 3-σ level in all the $C_t \lesssim 0$ region, for $C_V \simeq 1$ (as shown in the last column of table 5).

The five different channels are statistically independent by construction. No systematic uncertainties are estimated for the time being. Then, we obtained the 95% confidence-level (C.L.) upper limits on an anomalous cross section for $pp \to tqH$ by building a likelihood that is the product of the likelihoods for all channels. We report the results of our analysis in the (C_V, C_f) plane, in the two hypotheses where either a universal rescaling of the Higgs couplings to fermions is assumed ($C_f = C_t$), or C_t is a free parameter, and the remaining scaling factors are fixed to their SM value ($C_{f\neq t} = 1$). Figure 4 shows the exclusion contour in these two assumptions, along with the regions currently favored by the fits to present Higgs data in the universal scaling scenario [4, 6]. In both scenarios, the potential of the combination of the five channels considered here for the exclusion of the $C_t \lesssim 0$ region is quite remarkable. In particular, in the universal C_f scaling scenario, one can completely cover at this stage all the negative C_f space compatible with global fits.

It is also interesting to note a partial complementarity with the potential of the $H \to \bar{b}b$ channel, performed in [17]. In the universal rescaling hypothesis, the main sensitivity in the region $|C_t| \lesssim 1$ comes from the decays of the Higgs into bosons, as of the branching ratios of the Higgs to fermions (notably BR_{bb}) is depleted. Conversely, assuming $C_{f\neq t} = 1$, there is no large enhancement in the branching ratio of the Higgs to $WW^*, \tau\tau$ (and only a moderate increase in the $H \to \gamma\gamma$ rate, cf. figure 3), thus resulting in lower sensitivities. In both scenarios, the negative minimum lies well within the contours of the excluded region.

JHEP07(2013)073

	Channels					*Total*
Process	$\gamma\gamma bqqq'$	$\gamma\gamma b\ell q'$	$\ell_i^\pm\ell_i^\pm\ell_j^\mp bq'$	$\ell_i^\pm\ell_j^\pm\ell_j^\mp bq'$	$\ell^\pm\ell^\pm bqqq'$	
$\mathbf{C_t = -1.5}$						
S	2.6	2.4	0.91	2.4	3.6	11.9
B	1.04	0.73	0.86	2.7	14.3	19.6
$S/\sqrt{S+B}$	1.4	1.4	0.68	1.1	0.85	2.5
$\mathbf{C_t = -1}$						
S	2.8	2.5	0.81	2.2	6.6	14.9
B	1.02	0.60	0.83	2.6	14.0	19.1
$S/\sqrt{S+B}$	1.4	1.4	0.63	1.0	1.5	2.8
$\mathbf{C_t = 0}$						
S	2.3	2.0	0.70	1.8	5.4	12.2
B	0.97	0.23	0.65	2.2	12.2	16.2
$S/\sqrt{S+B}$	1.3	1.3	0.60	0.90	1.3	2.5
$\mathbf{C_t = 0.3}$						
S	1.0	0.80	0.33	0.84	2.5	5.5
B	0.98	0.29	0.70	2.3	12.7	17.0
$S/\sqrt{S+B}$	0.71	0.77	0.33	0.47	0.64	1.4

Table 5. Event rates (S) for the signal $p\,p \to t\,q\,H$, for different C_t values and $C_f = C_t$ (at $C_V \simeq 1$), in the five different final states corresponding to the decays $H \to \gamma\gamma$, WW^*, $\tau\tau$, with integrated luminosity of 50 fb^{-1} at 8 TeV. The corresponding background rates (B) and related significances are also detailed. The total significance (last column) is obtained by summing up in quadrature individual significances.

The parton level analysis performed here thus shows that studying the $p\,p \to t\,q\,H$ production in bosonic Higgs decays is the most sensitive approach for constraining an anomalous top-Higgs Yukawa coupling in the negative C_f region.

5 Conclusions

The sensitivity to an anomalous top Yukawa couplings of the single top and Higgs associated production $pp \to tqH$ has been assessed with the Higgs and the top quark decaying to the most robust final states (that is either resonant photon pairs or multi-lepton final states) for a luminosity of 50 fb^{-1} at 8 TeV collisions, roughly corresponding to the present data set collected by the ATLAS and CMS experiments. In particular, we extended our previous study in [16] by both complementing the $H \to \gamma\gamma$ analysis made for a hadronic top decay with a semi-leptonic top decay, and including multi-lepton final states originating by a Higgs decaying into WW^* and $\tau\tau$ pairs. Correspondingly, apart from the two-photon channels, we analyzed the three-lepton and two-same-sign-lepton signatures arising from

JHEP07(2013)073

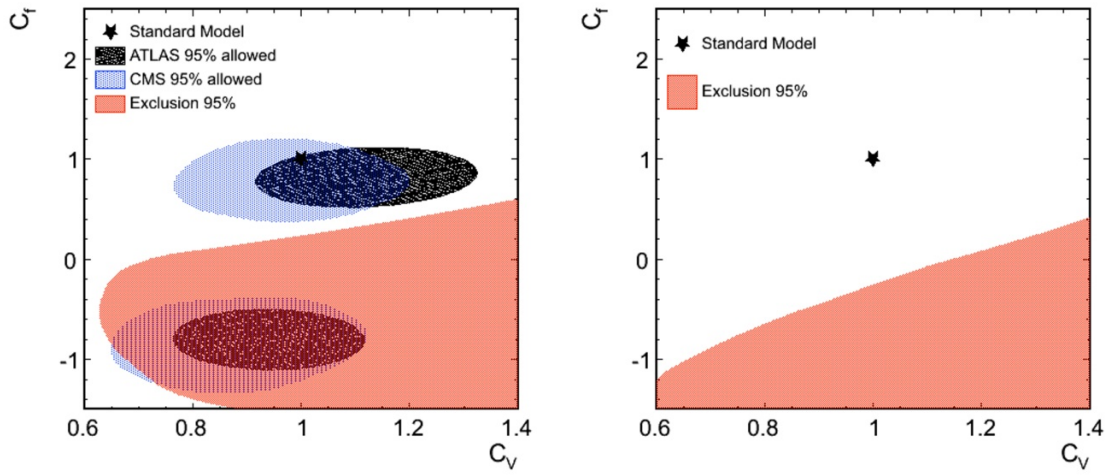

Figure 4. The left plot shows the (C_V, C_f) plane with the currently allowed parameter regions by the ATLAS (dark shaded oval) and CMS (light shaded oval) experiments [4, 6], in the universal C_f scaling assumption. The red dashed area corresponds to the 95% C.L. exclusion contours that can be achieved by searching for anomalous $p\,p \to t\,q\,H$ production with $H \to \gamma\gamma, WW^*, \tau\tau$, in 50 fb^{-1} of LHC data at 8 TeV. The right plot shows the 95% exclusion contour for a free C_t with $C_{f\neq t} = 1$. Negative-sign regions for the C_f scaling factor can be excluded in both scenarios.

the leptonic and semi-leptonic Higgs decay modes through WW^* and $\tau\tau$ pairs combined with the semi-leptonic top decays. We presented a parton-level analysis, and assumed the dominance of the corresponding *irreducible* backgrounds, which, for multi-photon and multi-lepton final states, is in general a reliable hypothesis. We anyhow also included a few backgrounds among the dominant reducible ones for the 2-photon final states.

Remarkably, we find that combining the aforementioned multiple final states, on the basis of the 50 fb^{-1} statistics already collected at 7 and 8 TeV collisions, an excess in the $pp \to tqH$ cross section could signal the presence of an anomalous top-Yukawa coupling with flipped sign with respect to the SM value. In the universal scaling hypothesis for the Yukawa sector, the non observation of such an excess could anyhow exclude at 95% of C.L. the reversed-sign region, in the (C_V, C_f) plane presently allowed by the combination of all Higgs measurements in other channels [4, 6]. In a scenario where the anomalous behavior is restricted to the top quark, the $pp \to tqH$ can still exclude values $C_t \lesssim -0.2$ for $C_V \simeq 1$. The potential of the considered signatures shows some complementarity with the $pp \to tqH$ potential in the $H \to \bar{b}b$ channel [17].

We then urge the ATLAS and CMS collaborations to perform our analysis in a more realistic environment, in order to either confirm or exclude the negative-sign region of the top Yukawa scaling factor, which is presently allowed by the ATLAS and CMS Higgs-coupling fits.

JHEP07(2013)073

Acknowledgments

S.B. would like to thank the cluster computing facilities of RECAPP, Harish-Chandra Research Institute. F.M. acknowledges the support of the "Rita Levi Montalcini" program at Ministero Istruzione Università e Ricerca. E.G. thanks the PH-TH division of CERN for its kind hospitality during the preparation of this work. This work was supported by the Estonian Science Foundation grant MTT60, by the recurrent financing SF0690030s09 project and by the European Union through the European Regional Development Fund.

References

[1] ATLAS collaboration, *Observation of a new particle in the search for the Standard Model Higgs boson with the ATLAS detector at the LHC*, *Phys. Lett.* **B 716** (2012) 1 [arXiv:1207.7214] [INSPIRE].

[2] CMS collaboration, *Observation of a new boson at a mass of* 125 *GeV with the CMS experiment at the LHC*, *Phys. Lett.* **B 716** (2012) 30 [arXiv:1207.7235] [INSPIRE].

[3] LHC Higgs Cross section Working Group collaboration, A. David et al., *LHC HXSWG interim recommendations to explore the coupling structure of a Higgs-like particle*, arXiv:1209.0040 [INSPIRE].

[4] ATLAS collaboration, *Coupling properties of the new Higgs-like boson observed with the ATLAS detector at the LHC*, ATLAS-CONF-2012-127, CERN, Geneva Switzerland (2012).

[5] ATLAS collaboration, *Combined coupling measurements of the Higgs-like boson with the ATLAS detector using up to* $25\,\text{fb}^{-1}$ *of proton-proton collision data*, ATLAS-CONF-2013-034, CERN, Geneva Switzerland (2013).

[6] CMS collaboration, *Combination of Standard Model Higgs boson searches and measurements of the properties of the new boson with a mass near* 125 *GeV*, CMS-PAS-HIG-12-045, CERN, Geneva Switzerland (2012).

[7] CDF and D0 collaborations, *Higgs boson studies at the Tevatron*, arXiv:1303.6346 [INSPIRE].

[8] J. Espinosa, C. Grojean, M. Muhlleitner and M. Trott, *Fingerprinting Higgs suspects at the LHC*, *JHEP* **05** (2012) 097 [arXiv:1202.3697] [INSPIRE].

[9] A. Azatov et al., *Determining Higgs couplings with a model-independent analysis of* $h \to \gamma\gamma$, *JHEP* **06** (2012) 134 [arXiv:1204.4817] [INSPIRE].

[10] P.P. Giardino, K. Kannike, I. Masina, M. Raidal and A. Strumia, *The universal Higgs fit*, arXiv:1303.3570 [INSPIRE].

[11] T. Alanne, S. Di Chiara and K. Tuominen, *LHC data and aspects of new physics*, arXiv:1303.3615 [INSPIRE].

[12] J. Ellis and T. You, *Updated global analysis of Higgs couplings*, *JHEP* **06** (2013) 103 [arXiv:1303.3879] [INSPIRE].

[13] A. Djouadi and G. Moreau, *The couplings of the Higgs boson and its CP properties from fits of the signal strengths and their ratios at the* $7+8$ *TeV LHC*, arXiv:1303.6591 [INSPIRE].

[14] A. Azatov and J. Galloway, *Electroweak symmetry breaking and the Higgs boson: confronting theories at colliders*, *Int. J. Mod. Phys.* **A 28** (2013) 1330004 [arXiv:1212.1380] [INSPIRE].

JHEP07(2013)073

[15] A. Falkowski, F. Riva and A. Urbano, *Higgs at last*, arXiv:1303.1812 [INSPIRE].

[16] S. Biswas, E. Gabrielli and B. Mele, *Single top and Higgs associated production as a probe of the $Ht\bar{t}$ coupling sign at the LHC*, *JHEP* **01** (2013) 088 [arXiv:1211.0499] [INSPIRE].

[17] M. Farina, C. Grojean, F. Maltoni, E. Salvioni and A. Thamm, *Lifting degeneracies in Higgs couplings using single top production in association with a Higgs boson*, *JHEP* **05** (2013) 022 [arXiv:1211.3736] [INSPIRE].

[18] W.J. Stirling and D. Summers, *Production of an intermediate mass Higgs boson in association with a single top quark at LHC and SSC*, *Phys. Lett.* **B 283** (1992) 411 [INSPIRE].

[19] A. Ballestrero and E. Maina, *$t\bar{b}H$ production for an intermediate mass Higgs*, *Phys. Lett.* **B 299** (1993) 312 [INSPIRE].

[20] G. Bordes and B. van Eijk, *On the associate production of a neutral intermediate mass Higgs boson with a single top quark at the LHC and SSC*, *Phys. Lett.* **B 299** (1993) 315 [INSPIRE].

[21] T.M. Tait and C.-P. Yuan, *Single top quark production as a window to physics beyond the Standard Model*, *Phys. Rev.* **D 63** (2000) 014018 [hep-ph/0007298] [INSPIRE].

[22] F. Maltoni, K. Paul, T. Stelzer and S. Willenbrock, *Associated production of Higgs and single top at hadron colliders*, *Phys. Rev.* **D 64** (2001) 094023 [hep-ph/0106293] [INSPIRE].

[23] V. Barger, M. McCaskey and G. Shaughnessy, *Single top and Higgs associated production at the LHC*, *Phys. Rev.* **D 81** (2010) 034020 [arXiv:0911.1556] [INSPIRE].

[24] J. Campbell, R.K. Ellis and R. Röntsch, *Single top production in association with a Z boson at the LHC*, arXiv:1302.3856 [INSPIRE].

[25] T. Appelquist and M.S. Chanowitz, *Unitarity bound on the scale of fermion mass generation*, *Phys. Rev. Lett.* **59** (1987) 2405 [*Erratum ibid.* **60** (1988) 1589] [INSPIRE].

[26] J. Alwall, M. Herquet, F. Maltoni, O. Mattelaer and T. Stelzer, *MadGraph 5: going beyond*, *JHEP* **06** (2011) 128 [arXiv:1106.0522] [INSPIRE].

[27] J. Pumplin et al., *New generation of parton distributions with uncertainties from global QCD analysis*, *JHEP* **07** (2002) 012 [hep-ph/0201195] [INSPIRE].

[28] CDF and D0 collaborations, *Combination of the top-quark mass measurements from the Tevatron collider*, *Phys. Rev.* **D 86** (2012) 092003 [arXiv:1207.1069] [INSPIRE].

[29] Particle Data Group collaboration, J. Beringer et al., *Review of particle physics (RPP)*, *Phys. Rev.* **D 86** (2012) 010001 [INSPIRE].

[30] A. Djouadi, J. Kalinowski and M. Spira, *HDECAY: a program for Higgs boson decays in the Standard Model and its supersymmetric extension*, *Comput. Phys. Commun.* **108** (1998) 56 [hep-ph/9704448] [INSPIRE].

[31] T. Sjöstrand, S. Mrenna and P.Z. Skands, *PYTHIA 6.4 physics and manual*, *JHEP* **05** (2006) 026 [hep-ph/0603175] [INSPIRE].

[32] CMS collaboration, *Measurement of associated production of vector bosons and top quark-antiquark pairs at $\sqrt{s} = 7$ TeV*, *Phys. Rev. Lett.* **110** (2013) 172002 [arXiv:1303.3239] [INSPIRE].

JHEP07(2013)073